UDC 621.313.335

ROBUST NEURO-FUZZY CONTROL OF HIGH DYNAMICS MOTORS FOR SURFACE POTENTIAL CARTOGRAPHY

A. Melahi[1], B. Bendahmane[2], B. Yahiaoui[3]

[1] *Laboratoire de maitrise des énergies renouvelables, Faculté de Technologie, Université de Bejaia, Algérie*
[2] *Laboratoire de Génie Electrique, Faculté de Technologie, Université de Bejaia, Algérie*
[3] *Département de Génie Electrique, Faculté de Technologie, Université de Bejaia, Algérie*

Abstract. *Within this paper, we present robust neuro-fuzzy control of motors with high dynamics to get 2D cartography of the potential obtained by corona discharge on the surface of materials. The system, controlled by robust H∞ controllers improved by neuro-fuzzy supervision, tracks predefined scanning trajectories giving the distribution of the surface potential and the potential decay with good performances.*

Key words: *H∞ robust control, Neuro-fuzzy control, Scanning trajectories, Cartography, Surface potential distribution, Surface potential decay, Corona discharge*

Introduction

Surface potential cartography using a moving probe on the surface of a material (PVC for example) permits to have the distribution of the potential on the charged surfaces by corona discharge that make possible predictions on the distributions of the electric charges (electrets) on that surface. The charged surfaces are used in several domains. The characterization of the electrets gives certain classifications of the several materials used in this domain and it is studied using specific systems performing the measure of the surface potential on certain predefined points or trajectories and doing reconstitution of the surface potential distribution in 2-dimensions.

Known that the potential on the surface may change (potential decay) because of the displacement of the electric charges on the surface [1], the cartography has to be done quickly and confidently. In this objective, the use of high dynamics positioning system is necessary.

Several systems were used in this field of high dynamics motion control. In addition, different techniques of control were proposed, like robust control, which take into account the presence of the disturbances during the design of the regulators [5, 12, 17, and 18].

Fuzzy control and neuro-fuzzy control can make model reference adaptive control that can learn and adjust their parameters in order to get the wanted performances [3, 6, 7, 8, 9, 10, 11, 13, and 14].

In this work, the reference models are first order systems with unitary gain and time constant to be chosen adequately to perform the tasks at hand (scanning, measuring, reconstitution).

© Melahi A., Bendahmane B., Yahiaoui B. 2018

1. Description of the system

The system has three sub-systems: the first for the corona discharge process, the second for the scanning operation and the third for the neutralization process. The figure below fig.1 gives a 3D virtual presentation of the system where the focus is on the scanning operation sub-system.

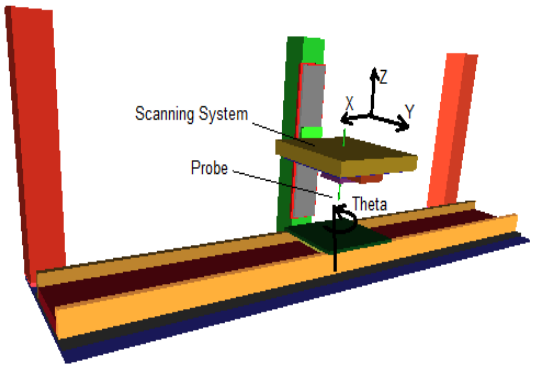

Fig. 1. 3D virtual presentation of the system

At first, we place the plate in the first sub-system in order to charge the surface of the plate and have a surface potential distribution. After, the plate passes to the second sub-system in order to perform the scanning operation. Finally, the plate goes to the third sub-system for neutralization.

We use two methods for corona discharge: point-plate and axis-plate as presented in the figure fig.2 (the grid between the electrode and the plate is omitted for simplicity). The plate is a square material sample (10 cm x 10 cm). Typical obtained potential distributions are given in the figure fig.3.

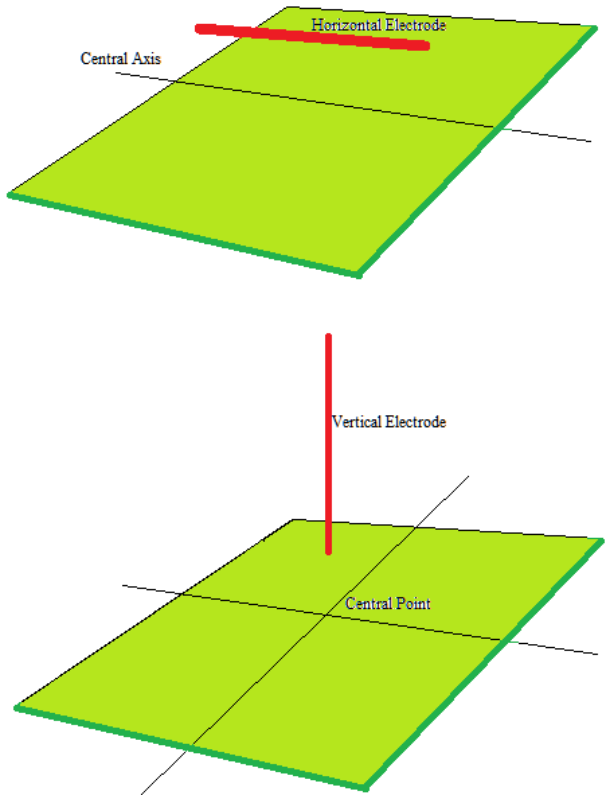

Fig. 2. Corona discharge methods (axis-plate) and (point-plate)

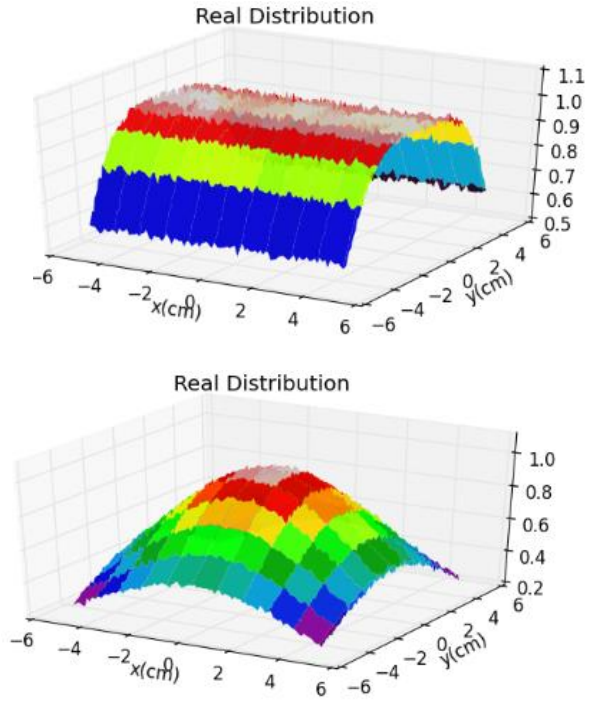

Fig. 3. Typical potential distributions obtained by corona discharge (axis-plate) and (point-plate)

The scanning sub-system has four dc-motors (axes: X, Y, Z and θ). The θ-axis orientates the plate in order to be parallel to the XY-axes. The Z-axis places the probe over the plate at a fixed height (about 3mm). The XY-axes perform the scanning operation and have both high dynamics dc-motors.

The surface potential measured by the probe centered at (x_p,y_p), is given by:

$$SP(x_p, y_p) = Gp \,.\, Mp \tag{1}$$

$$Mp = \frac{\iint D_r(x,y) \cdot D_p(x - x_p, y - y_p) \cdot dx \cdot dy}{\iint D_r(x,y) \cdot dx \cdot dy} \tag{2}$$

Where *Gp* stands for the transfer function (temporal filter) and *Mp* is the weighed sum over the material surface of the real surface potential distribution D_r and D_p is the spatial filter of the probe.

2. X-Y Positioning system

The X-Y positioning system as presented in the figure fig.4 is a two sub-systems of double integrators with electric and mechanical disturbances. The disturbances present the effects of extern resistant torque, and the incertitude in the dc-motors parameters (inertia J, friction f, gain K and so on). The design the H∞ robust control uses this representation to have the LFT form (Linear Fractional Transform form).

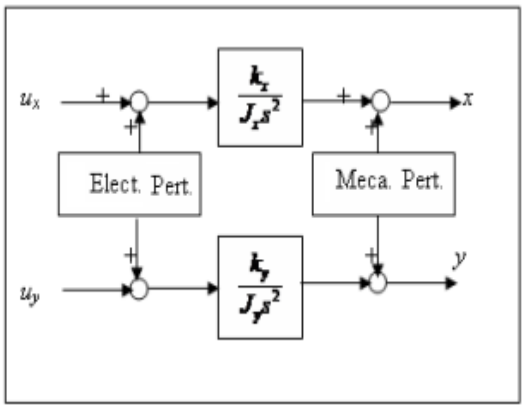

Fig. 4. Simplified model of high dynamics dc-motors with mechanical and electric disturbances

3. Positioning System Control

The closed loop system is presented in the figure below (fig.5). The controller *K* is a robust H∞ controller that rejects the effects of the disturbances δe and δs. The neuro-fuzzy controller is adaptive with the back-propagation learning algorithm to adjust the parameters of the Sugeno-type fuzzy controller. The objective of this adjustment is to minimize the difference between the output of the system *S* and the output of the reference model *Sm*.

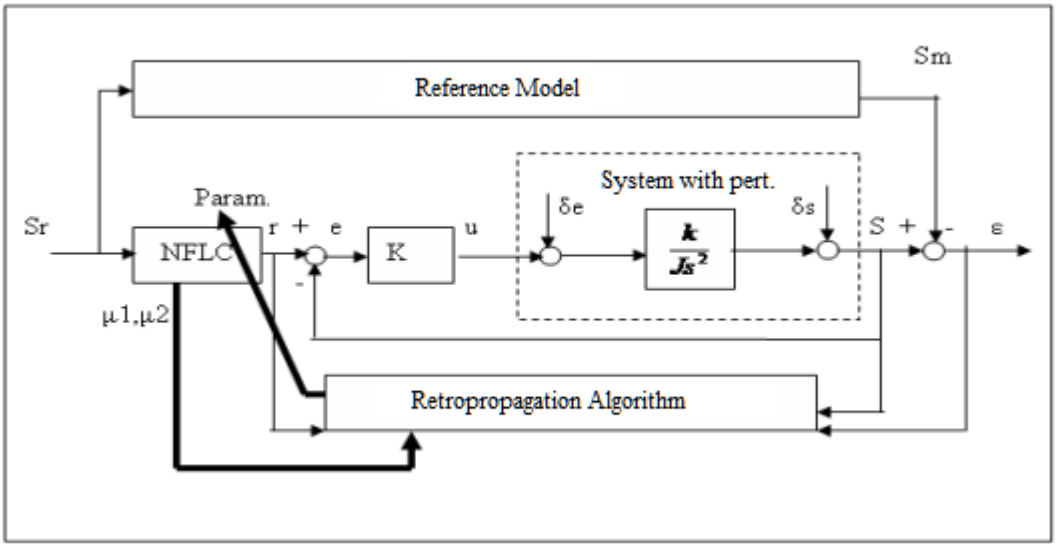

Fig. 5. The control system

The Sugeno-type fuzzy controller calculates the modified reference input *r*:

$$r = NFLC(Sr) \tag{3}$$

$$r = \frac{\mu_1(Sr)\cdot f_1(Sr) + \mu_2(Sr)\cdot f_2(Sr)}{\mu_1(Sr) + \mu_2(Sr)} \tag{4}$$

Where the membership functions are:

$$\mu_1(Sr) = e^{-((Sr+m)/\sigma)^2} \tag{5}$$

$$\mu_2(Sr) = e^{-((Sr-m)/\sigma)^2} \tag{6}$$

The consequences of the rules are:

$$f_1(Sr) = a_1 \cdot Sr + b_1 \tag{7}$$

$$f_2(Sr) = a_2 \cdot Sr + b_2 \tag{8}$$

The back-propagation algorithm gives the learning formulas updating the parameters *m, σ, a_1, a_2, b_1 and b_2*:

$$\dot{m} = -\eta_m \cdot \left\{ \left[\frac{2}{\sigma^2} \cdot \varepsilon \cdot \frac{\Delta S}{\Delta r} \cdot \frac{f_1 \cdot \mu_1 + f_2 \cdot \mu_2}{(\mu_1 + \mu_2)^2} \right] \cdot \right. \\ \left. \cdot \left[(Sr - m)\cdot \mu_2 + (Sr + m)\cdot \mu_1 \right] \right\} \tag{9}$$

$$\dot{\sigma} = -\eta_\sigma \cdot \left\{ \left[\frac{2}{\sigma^3} \cdot \varepsilon \cdot \frac{\Delta S}{\Delta r} \cdot \frac{f_1 \cdot \mu_1 + f_2 \cdot \mu_2}{(\mu_1 + \mu_2)^2} \right] \cdot \right. \\ \left. \cdot \left[(Sr - m)^2 \cdot \mu_2 - (Sr + m)^2 \cdot \mu_1 \right] \right\} \tag{10}$$

$$\dot{a}_1 = \eta_{a_1} \cdot Sr \cdot \rho_1 \cdot \varepsilon \cdot \frac{\Delta S}{\Delta r} \tag{11}$$

$$\dot{b}_1 = \eta_{b_1} \cdot \rho_1 \cdot \varepsilon \cdot \frac{\Delta S}{\Delta r} \tag{12}$$

$$\dot{a}_2 = \eta_{a_2} \cdot Sr \cdot \rho_2 \cdot \varepsilon \cdot \frac{\Delta S}{\Delta r} \tag{13}$$

$$\dot{b}_2 = \eta_{b_2} \cdot \rho_2 \cdot \varepsilon \cdot \frac{\Delta S}{\Delta r} \tag{14}$$

$$\begin{cases} \varepsilon = Sm - S \\ \rho_1 = \dfrac{\mu_1}{\mu_1 + \mu_2} \\ \rho_2 = \dfrac{\mu_2}{\mu_1 + \mu_2} \end{cases} \tag{15}$$

4. Reference trajectories

Several trajectories for the scanning operation are proposed. We used back and forth trajectory, Lissajous curves trajectory and random trajectory (normal distribution).

The first trajectory is point-to-point movements with a constant speed and one axis in motion at a time. The second trajectory follows the equations below.

$$\begin{cases} X(\theta) = X_m \cdot \cos(n \cdot \theta) \\ Y(\theta) = Y_m \cdot \cos(m \cdot \theta + \varphi) \end{cases} \tag{16}$$

Where

$$\dot{\theta} = V \cdot \left(X_m^2 n^2 \sin^2(n\theta) + Y_m^2 m^2 \sin^2(m\theta + \varphi) \right)^{-\frac{1}{2}} \quad (17)$$

And

$$\theta(t) = \theta(0) + \int_0^t \dot{\theta}(t) \cdot dt \quad (18)$$

The variable V stands for the probe constant speed (positive) on the trajectory and n, m (positive integers) and φ are well chosen to get Lissajous curves.

The third trajectory is point-to-point movements where the points are chosen randomly (with normal distribution) over the [-5 cm, +5 cm] x [-5 cm, +5 cm] square.

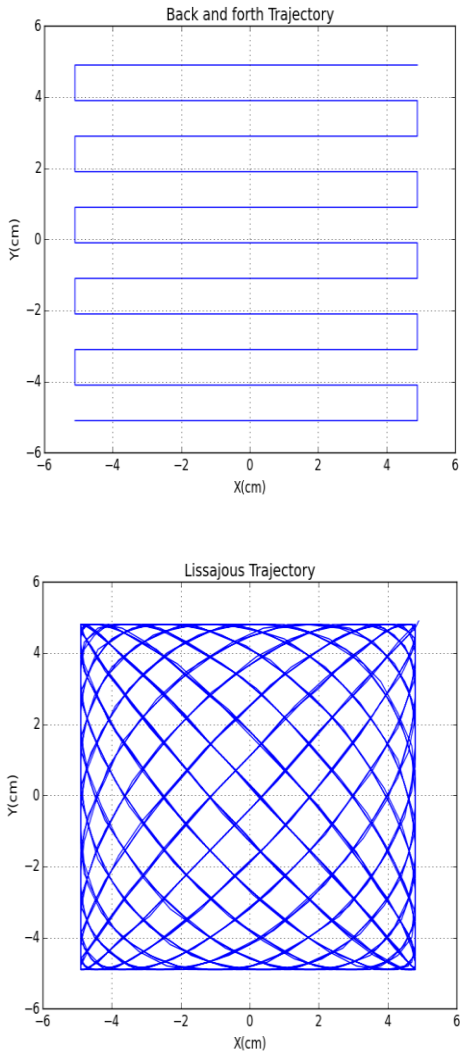

Fig. 6. Scanning trajectories (back and forth, Lissajous)

5. Reference model

With the presence of the potential decay, we must perform rapid scanning in order to have several cartographies of the potential on the surface of the material. We take the case where the potential decay has 15 minutes (900 seconds) to stabilize at its final value [1].

The reference model is a first order system with unitary gain and time constant τ.

In order to have several cartographies and given that the speed of the probe displacement and the length of the trajectories are constants, one can take different values for the time constant τ.

6. Simulation results

The simulations conducted using Matlab and Python programming languages give the results presented in the figures below (from fig.7 to fig.14). We class these results under two sub-classes: slow scanning and rapid scanning.

We use the slow scanning to visualize the potential decay (increased by 15 times in the figures below: fig.7 – fig.9) where we can see the evolution of the surface potential at several selected points on the surface of the material.

The figures fig.7, fig.8 and fig.9 state that when doing the scanning, the potential on the surface changes rapidly with respect to the scanning operation. Here we cannot do the reconstitution of the surface potential but we still can use the results to present the potential decay because of the constant speed (low speed) of the scanning operation.

The difference between fig.7 and figures fig.8 and fig.9 is that we do one pass over the trajectory in figure fig.7 and several passes over the trajectory of figures fig.8 and fig.9.

In fig.7, we suppose that the surface potential distribution is homogenous over the surface and has the same behavior on all straight lines that are parallel to electrode axis in the case of the axis-plate distribution. This method gives a general aspect of the evolution of the surface potential and is not very accurate because the potential is measured at several points (considered as the same point). We cannot use this technique to visualize the potential decay with the point-plate distribution.

However, for the figures fig.8 and fig.9, the probe performs several passes on the trajectory and we can visualize the potential decay in any point on the trajectory as shown in these figures.

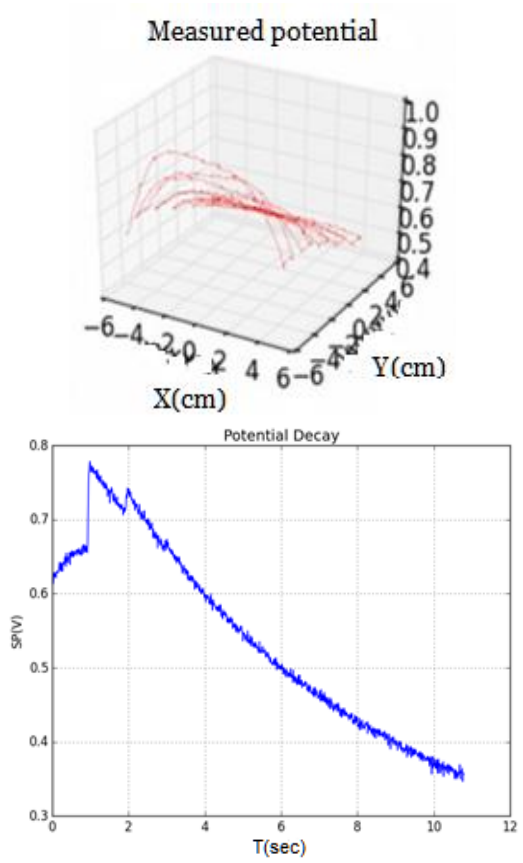

Fig. 7. Potential decay with slow scanning, back and forth trajectory and axis-plate corona discharge

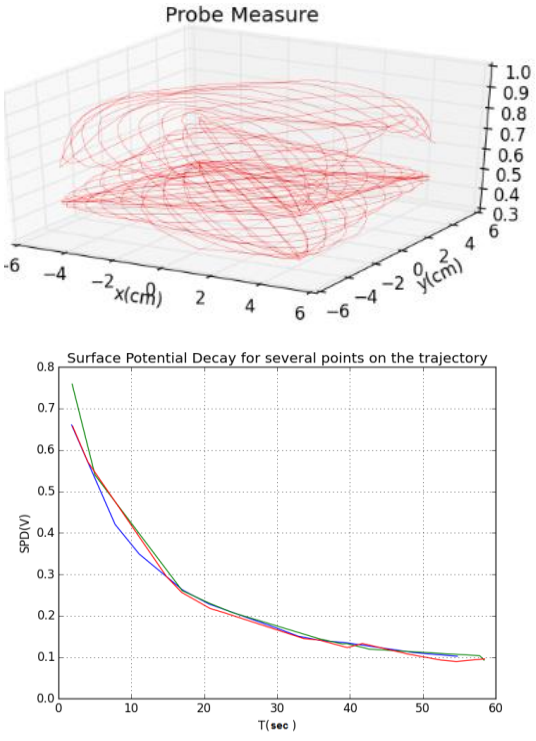

Fig. 8. Potential decay with slow scanning, Lissajous trajectory and axis-plate corona discharge

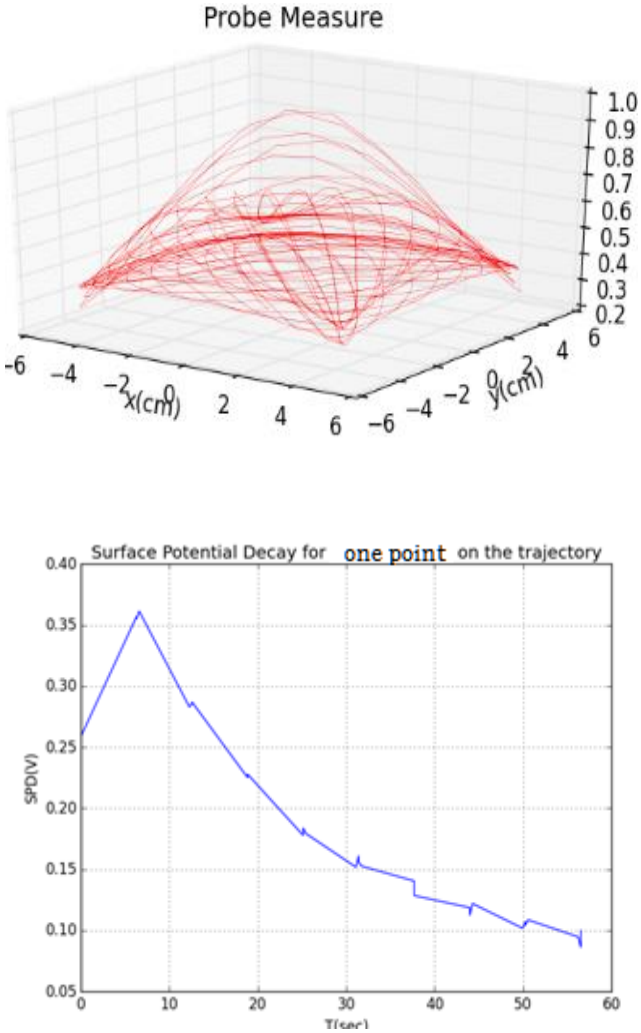

Fig. 9. Potential decay with slow scanning, Lissajous trajectory and point-plate corona discharge

For the figures fig.10 through fig.15, we can see the measured potential on the trajectories, the reconstitution of the surface potential distribution and the error of the reconstitution. We, first, have done the reconstitution by taking all the measures (about 1000 samples) but we noticed that a random choice over the samples permits to do the reconstitution with 60-to-100 samples. Therefore, we have limited the reconstitution to use just 60-to-100 samples. This idea conducted us to use the method of the random trajectory that chooses randomly 60-to-100 points on the surface and performs the point-to-point motion. This has led to the shortest time scanning operation.

As we can see, the error of the reconstitution is very small and that depends on good scanning and the method used for reconstitution. We used the Least Squares Method and a 12-degree polynomial on *X* and *Y* (6 degrees for both).

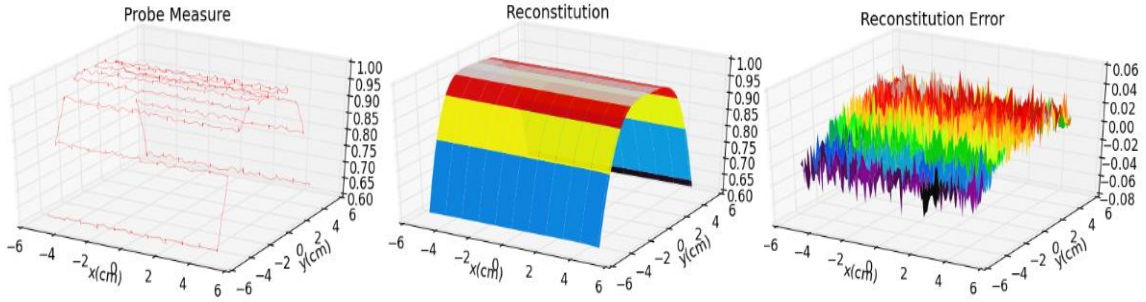

Fig. 10. Surface Potential distribution with rapid scanning, back and forth trajectory and axis-plate corona discharge (measure, reconstruction and error of reconstruction)

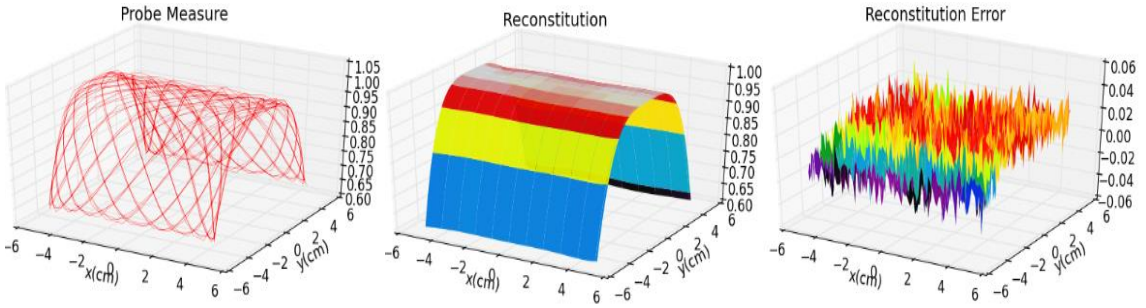

Fig. 11. Surface Potential distribution with rapid scanning, Lissajous trajectory and axis-plate corona discharge (measure, reconstruction and error of reconstruction)

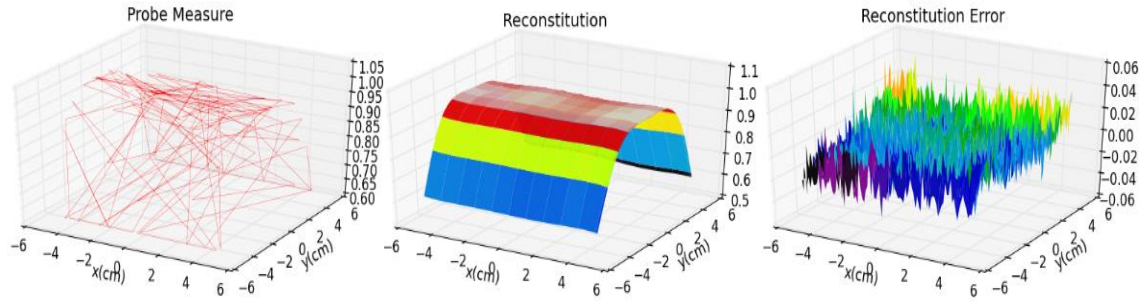

Fig. 12. Surface Potential distribution with rapid scanning, random trajectory and axis-plate corona discharge (measure, reconstruction and error of reconstruction)

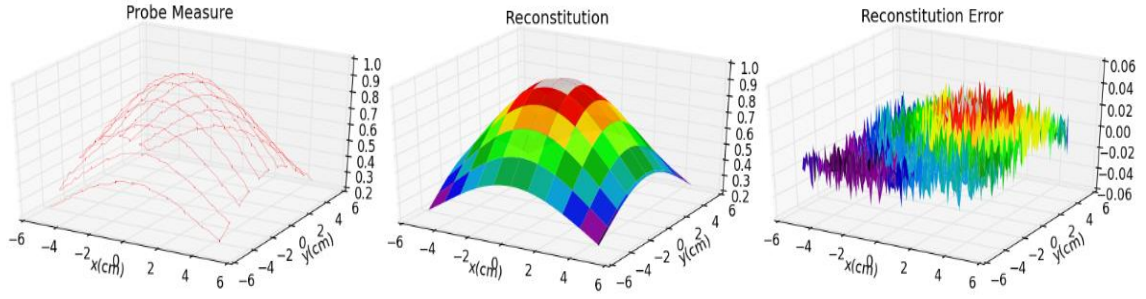

Fig. 13. Surface Potential distribution with rapid scanning, back and forth trajectory and point-plate corona discharge (measure, reconstruction and error of reconstruction)

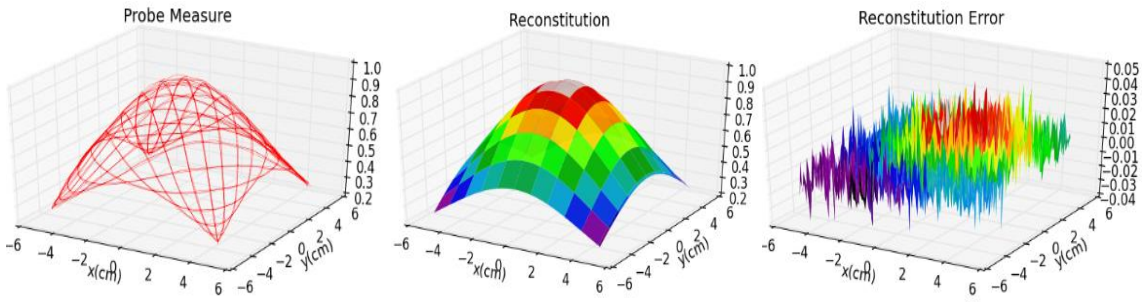

Fig. 14. Surface Potential distribution with rapid scanning, Lissajous trajectory and point-plate corona discharge (measure, reconstruction and error of reconstruction)

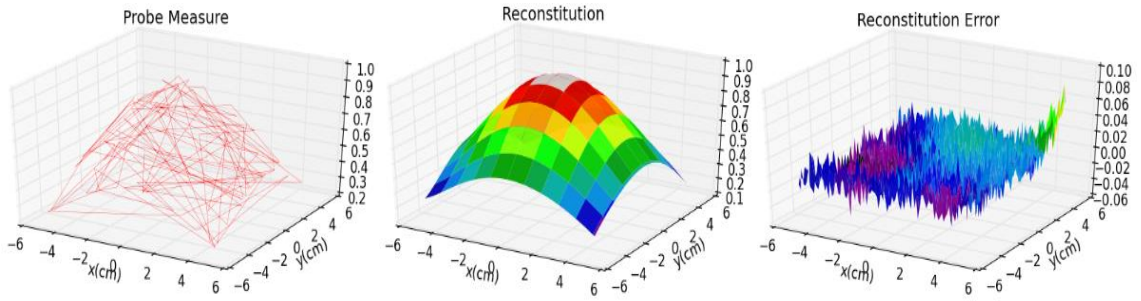

Fig. 15. Surface Potential distribution with rapid scanning, random trajectory and point-plate corona discharge (measure, reconstruction and error of reconstruction)

7. Discussion

We took the reference model as a first order system with unitary static gain and time constant τ=0.1sec.

For the back and forth trajectory, we found that one cartography is done in 100 seconds and that allows us to make approximately 7 cartographies in 900 seconds (15 minutes, the potential decay duration).

For the Lissajous trajectory, we have 10 seconds per cartography and that allows us to get about 70 cartographies in 900 seconds.

The random trajectory gives the shortest time per cartography (1 second).

Using curve-fitting techniques, one can perform the reconstitution of the surface potential. We used the Least Square Method and a 12 order polynomial in X and Y (X and Y are at 6 degrees both). In addition, we found that 60 through 100 samples permit the reconstitution of the surface potential this way.

The fact that 60 through100 samples permit the reconstitution of the surface potential justifies the results given by the scanning using the random trajectory. We have to move the probe to just 60 through 100 points randomly chosen on the plate (slab).

With several cartographies, we can realize animations to visualize the time evolution of the surface potential distribution.

Conclusion

In this work, we have designed robust neuro-fuzzy controllers in order to move a probe that measures the potential on a plate (surface) caused by the corona discharge. The robust controller reduced the disturbance effects, and it did not permit to impose certain wanted dynamics. The use of the fuzzy control solved this problem by modifying the reference signal in order to track a reference model. The neuro-fuzzy approach allowed us to improve the tracking of the reference model and adaptively adjusted (on line) the parameters of the fuzzy controller. Indeed, the neuro-fuzzy controller supervises the robust controller by generating the adequate reference signal that permits to minimize the error signal between the output of the system and the output of the reference model.

The use of different trajectories showed that we could do several tasks: potential decay visualization, surface potential distribution reconstruction and animation to visualize the time evolution of the surface potential distribution.

The slow scanning operation permitted the visualization of the potential decay and the rapid

scanning operation allowed having the distribution of the potential on the surface of the plate.

In order to produce the animation, the probe must do several cartographies. Our work showed that the random trajectory permits to have the shortest time scanning per cartography.

The choice of the time constant of the reference model is typically 0.1 second (tests were conducted for other values).

The extensive conducted simulations confirm and validate the approach.

Acknowledgements

We thank Mr. Lucien Dascalescu from Poitiers University, France and our colleague Mr. Belaid Tabti, the initiators of this work. Our thanks goes to Mr. Marian Bogdan Neagoe from Poitiers University, France, for the several discussions and comments on this work.

References

1. B. Tabti, (2011) "Contributions à la caractérisation des filtres à électret par la mesure du déclin de potentiel de surface", Thèse de doctorat, Université de Poitiers.

2. W. Khalil, E. Dombre, (1999) "Modélisation, identification et commandes des robots", Edition Hermes.

3. J. Wang, H. V. Brussel, J. Swevers, (1995) "Extended pole placement method with noncasual reference model for digital servo control", Trans. Of the ASME J. of Dynamic Systems, Measurement, and control, no.117, pp. 641–644.

4. Y.-T. Tseng, J.-H. Liu, (2003) "High-speed and precise positioning of an X-Y table, Elsevier: Control Engineering Practice", Vol. 11, pp. 357–365.

5. K. Pietrusewicz, (2012) "Multi-dgre of freedom robust control of the CNC X-Y table PMSM-based feed-drive module", Archives of Electrical Engineerineg, Vol. 61, no. 1, pp. 15–31.

6. M. Khadjoudj, N. Golea, M. E.-H. Benbouzid, (2007) "Fuzzy-rule based model reference adaptive control for PMSM drives", Serbian Journal of Electrical Engineering, Vol.4, no.1, pp. 13–22.

7. N. J. Patil, R. H. Chile, L. M. Waghmare, (2010) "Fuzzy adaptive controllers for speed control of PMSM drive", International Journal of Computer Applications, Vol. 1, no. 11, pp. 84–91.

8. A. Meroufel, M. Massoum, B. Belabbes, (2009) "Model reference adaptive fuzzy controller for permanent magnet synchronous motor", Mediamira Science Publisher, Vol. 50, no. 1, pp. 25–30.

9. Ch. U. M. Rao, B. M. Krishna, A. L. Soundarya, N. K. Kumari, (2015) "Field oriented control of PMSM with model reference adaptive control using fuzzy-PI controller", IJCTA, Vol. 8, no. 1, pp. 96–108.

10. R.J. Prabhu, S. Saravanan, S.C. Vijayakumar, (2013) "Adaptive control of stepping motors using artificial neural networks", IJESIT, Vol. 2, no. 4, pp. 228–232.

11. R. Jahani, H. C. Nejad, H. A. Shayanfar, A. Zare, (2010) "Positioning control of PM stepper motor based on type-2 fuzzy robust control", IJTPE, Vol. 2, Issue 5, no. 4, pp. 19–26.

12. L. Xu, B. Yao, (2001) "Output feedback adaptive robust precision motion control of linear motors", Automatica 37, pp. 1029–1039.

13. S. Z. Moussavi, M. Alasvandi, S. Javadi, E. Morad, (2014) " PMDC motor speed control optimization by implementing ANFIS and MRAC", IJCSE, pp. 1–8.

14. K. Keerthi, M.S. Sathyanarayana, (2012) "Fuzzy implementation of model reference adaptive control of DC drives, IJESAT, Vol. 2, Issue 3, pp. 605–611.

15. H. Yajima, H. Wakiwaka, K. Minegishi, N. Fujiwara, K. Tamura, (2000) "Design of linear DC motor for high-speed positioning", Elsevier: Sensors and Actuators 81, pp. 281–284.

16. G. Shahgholian, M. Maghsoodi, J. faiz, (2016) "Analysis of speed control in DC Motor drive based on model reference adaptive control", JPECS, Vol. 1, no. 2, pp. 66–71.

17. B. Yao, M. Al-Majed, M. Tomizuka, (1997) "High-performance robust motion control of machine tools: An adaptive robust control approach and comparative experiments", IEEE/ASME Trans. Mechatronics, Vol. 2, n°2, pp. 63–76.

18. N. H. Giap, J.-H. Shin, W.-H. Kim, (2013) "Robust adaptive neural network control for X-Y table, Intelligent Control and automation", vol. 4, pp. 293–300.

19. Q. Gu1, Y. Li,P. Niu1, J. Sun, (2014) "Optimized Design of SoC-based Control System for Multi-axis Drive", ELEKTRONIKA IR ELEKTROTECHNIKA, Vol. 20, no. 7, pp. 15–22.

20. J. U. Cho, Q. N. Le and J. W. Jeon, (2009) "An FPGA-based multiple-axis motion control chip", IEEE Trans. Ind. Electron., vol. 56, no.3, pp.856–870.

НАДІЙНИЙ НЕЙРОФУЗИЙ КОНТРОЛЬ ВЕЛИКИХ ДИНАМІЧНИХ МОТОРІВ ДЛЯ ПОТЕНЦІАЛЬНОЇ ПОВЕРХНЕВОЇ КАРТОГРАФІЇ

А. Мелахі[1], Б. Бендхман[2], Б. Яхіауі[3]

[1] Лабораторія майстерності відновлюваних джерел енергії, Технологічний факультет, Університет Беджіа, Алжир
[2] Лабораторія електротехніки, факультет технологій, Університет Беджіа, Алжир
[3] Кафедра електротехніки, Технологічний факультет, Університет Беджіа, Алжир

Анотація. *У цій роботі ми представляємо надійний нейро-нечіткий контроль двигунів з високою динамікою в цілях реалізації двовимірної картографії потенціалу на поверхні матеріалів, отриманих коронним розрядом. Система, підконтрольна ПК, має чотири DC-двигуни з високою динамікою (осей: X, Y, Z і θ) контролерами потужними контролерами H∞, покращеними за допомогою нейро-нечіткого нагляду. Ця система спрямована на відстеження заздалегідь заданих траєкторій сканування, щоб мати хороші відображення розподілу поверхневого потенціалу. Поверхня матеріалу паралельна площині XY, а траєкторії сканування виконані в цій площині. Запропоновані різні траєкторії сканування (вперед і назад, Lissajous, випадкові з нормальним розподілом). Ми проводимо відстеження з двома швидкостями: швидке відстеження та повільний відстеження. Швидке відстеження дозволяє мати декілька картографічних даних, перш ніж можуть з'явитися наслідки потенційного розпаду. Повільне відстеження дає час еволюції потенційного розпаду. Ми використали два еталонні розподіли, отримані: коронним розрядом точка-пластинки та коронним розрядом на осі. Проведене моделювання з використанням Python та Matlab показують різні форми картографії розподілу потенціалу поверхні. Коли сканування закінчене, отримані заходи дають потенціал по траєкторіях та за методами криволінійної обробки, ми отримуємо 2-мірний розподіл вимірюваного поверхневого потенціалу. Цей поверхневий потенціал відрізняється від реального потенціалу поверхні, з огляду на те, що використовуваний зонд на додаток до свого тимчасового фільтра має 2-мірний просторовий фільтр. Більше того, для реального розподілу поверхневого потенціалу ми повинні використовувати просторову деконволюцію, використовуючи просторовий фільтр зонда та отриманий вимірюваний розподіл поверхневого потенціалу. Метою даної роботи є отримання реального розподілу поверхневого потенціалу за допомогою швидкого сканування та розпаду поверхневого потенціалу за допомогою повільного сканування. Ці цілі ми отримуємо завдяки хорошим характеристикам використовуваних потужних нейро-нечітких контролерів та використанням двигунів високої динаміки. Завдяки швидкому скануванню ми можемо отримати декілька картографій та візуалізувати часові еволюції поверхневого потенціалу. При повільному скануванні ми можемо візуалізувати поверхневий потенціал розкладання часу-еволюції в будь-якій точці траєкторій, враховуючи те, що ми робимо кілька проходів.*

Ключові слова: *система позиціонування X-Y, надійний контроль H∞, нейро-нечіткий контроль, траєкторії сканування, картографія, розподіл потенціалу поверхні, розпад потенціалу поверхні, коронний розряд*

НАДЕЖНЫЙ НЕЙРОФУЗИЙ КОНТРОЛЬ ВЫСОКИХ ДИНАМИЧЕСКИХ МОТОРОВ ДЛЯ ПОВЕРХНОСТНОЙ ПОТЕНЦИАЛЬНОЙ КАРТОГРАФИИ

А. Мелахи[1], Б. Бендахман[2], Б. Яхияуи[3]

[1] Laboratoire de maitrise des énergies renouvelables, Факультет технологии, Университет де Беджая, Алжир
[2] Laboratoire de Génie Electrique, Факультет технологии, Университет де Беджая, Алжир
[3] Département de Génie Electrique, Факультет технологии, Университет де Беджая, Алжир

Аннотация. *В этой статье мы представляем надежное нейро-нечеткое управление двигателями с высокой динамикой, чтобы получить двумерную картографию потенциала, полученного коронным разрядом на поверхности материалов. Система, контролируемая мощными*

контроллерами H∞, улучшенная нейро-нечетким контролем, отслеживает предопределенные траектории сканирования, дающие распределение поверхностного потенциала и потенциального распада с хорошими характеристиками.

Ключевые слова: *устойчивое управление H∞, нейро-нечеткое управление, сканирующие траектории, картография, распределение поверхностного потенциала, разложение поверхностного потенциала, разложение короны*

Received 24.03.2018

Melahi Ahmed, PhD student , Enseignant-chercheur, Laboratoire de Maitrise des Energies Renouvelables, Faculté de Technologie, Université de Bejaia, Algeria, E-mail: melahi_ahmed@yahoo.fr, Tel: +213-055-119-88-67

Мелахі Ахмед, аспирант, викладач-дослідник, Лабораторія майстерності відновлюваних джерел енергії, Технологічний факультет, Університет Беджіа, Алжир, E-mail: melahi_ahmed@yahoo.fr, Тел: + 213-055-119-88-67

ORCID ID : 0000-0002-7686-0942

Bendahmane Boukhalfa, Ph.D, Senior Lecturer classe A, Directeur du Laboratoire de Génie Electrique, Faculté de Technologie, Université de Bejaia, Algeria, E-mail : bouxalfa_fr@yahoo.fr, Tel : +213-055-342-38-19

Бендхман Бухалфа, доктор доктор технических наук, науковий співробітник, директор лабораторії електротехніки, факультет технологій Алжирського університету в Беджіа, електронна адреса: bouxalfa_fr@yahoo.fr, тел .: + 213-055-342-38-19

ORCID ID : 0000-0002-5626-0093

Yahiaoui Belkacem, PhD, Enseignant-chercheur, Département de Génie Electrique, Faculté de Technologie, Université de Bejaia, Algeria, E-mail: bel.yahiaoui@gmail.com, Tel : +213-054-143-96-58

Яхіяуі Белкасем, PhD, вчитель-дослідник, дерартамент электротехники, факультет технології, Університет Беджіа, Алжир, електронна адреса: bel.yahiaoui@gmail.com, тел: + 213-054-143-96-58

ORCID ID : 0000-0002-8970-1975